

# Scaling of the island density and island-size distribution in irreversible submonolayer growth of three-dimensional islands

Y. A. Kryukov\* and J. G. Amar†

*Department of Physics and Astronomy, University of Toledo, Toledo, Ohio 43606, USA*

(Received 29 January 2010; revised manuscript received 6 April 2010; published 26 April 2010)

Motivated by observations of three-dimensional (3D) island formation in a variety of experiments, we have carried out kinetic Monte Carlo simulations of a simplified model of 3D island growth with critical island size  $i=1$  (irreversible growth). Of particular interest are the exponents  $y_1$  and  $y'_1$  describing the dependence of the submonolayer island density in the precoalescence regime on dose and coverage respectively, as well as the exponent  $\chi'_1$  describing the dependence of the peak island density on the ratio  $D/F$ , where  $D$  is the monomer hopping rate and  $F$  is the (per site) deposition rate. We find that the values of  $y_1$  and  $y'_1$  (e.g.,  $y_1 \approx 0.24$ ,  $y'_1 \approx 0.32$ ) are significantly lower than the standard rate-equation (RE) predictions ( $y_1=1/3$ ,  $y'_1=3/7 \approx 0.43$ ). This may be explained by the fact that, in contrast to the standard RE assumption of size-independent capture numbers, for 3D islands the island radius increases with the number of atoms in an island. Accordingly, the average capture number increases with coverage and as a result, the coverage dependence of the island density for 3D islands is intermediate between that for two-dimensional (2D) islands ( $y_1=y'_1=0$ ) and the standard RE prediction. As a result, the measured value of  $\chi'_1$  ( $\chi'_1 \approx 0.30$ ) is slightly larger than the standard RE prediction ( $\chi'_1=2/7 \approx 0.29$ ) but still lower than the value ( $\chi_1=1/3$ ) for irreversible 2D island growth. For comparison with our simulations we also present self-consistent RE results for the island and monomer densities as a function of coverage and excellent agreement is obtained without any adjustable parameters. Results for the scaled island-size distribution (ISD) for 2D and 3D irreversible island growth are also presented. Somewhat surprisingly, we find that there is very little difference between the scaled ISD for 3D islands and that for 2D islands. In addition to our simulation results, the scaling behavior of the 3D island density for general critical island size  $i$  is also discussed. Our results suggest that while the exponent  $\chi'_1$  describing the flux dependence of the peak island density is the most accurate indicator, the exponent  $y_i$  may also be useful to estimate the critical island size  $i$  in submonolayer 3D growth.

DOI: [10.1103/PhysRevB.81.165435](https://doi.org/10.1103/PhysRevB.81.165435)

PACS number(s): 81.15.Aa, 68.55.A-

## I. INTRODUCTION

The ordering and size distribution of islands in submonolayer growth plays an important role in determining the later stages of thin-film growth.<sup>1-5</sup> Accordingly, during the past few years considerable experimental and theoretical efforts<sup>6</sup> has been devoted to studying the dependence of the submonolayer scaling behavior on deposition conditions. Of particular interest is the dependence of the (per site) island density  $N$  and island-size distribution (ISD)  $N_s(\theta)$  (where  $N_s$  is the number density of islands of size  $s$  at coverage  $\theta$ ) on such deposition parameters as the deposition flux  $F$  and growth temperature  $T$ .

One concept that has proven especially useful is that of a critical island size, corresponding to one less than the size of the smallest “stable” cluster. For example, in the case of submonolayer growth of two-dimensional (2D) islands on a 2D substrate, standard nucleation theory<sup>2,3</sup> predicts that the peak island density satisfies

$$N_{pk} \sim (D/F)^{-\chi_i} e^{E_b/(i+2)k_B T}, \quad (1)$$

where  $D=D_0 e^{-E_a/k_B T}$  is the monomer hopping rate,  $E_a$  is the activation energy for monomer diffusion,  $E_b$  is the binding energy of the critical nucleus,  $i$  is the critical island size, and  $\chi_i = \frac{i}{i+2}$ . In addition, it has been shown that in the precoalescence regime the ISD satisfies the scaling form<sup>7,8</sup>

$$N_s(\theta) = \frac{\theta}{S^2} f_i\left(\frac{s}{S}\right), \quad (2)$$

where  $S$  is the average island size and the scaling function  $f_i(u)$  depends on the critical island size.<sup>9</sup>

While much of the theoretical work has focused on an analysis of the scaling behavior in the case of homoepitaxial 2D island growth or on quantum dot formation in the case of heteroepitaxial growth,<sup>10</sup> in some cases three-dimensional (3D) islands may also be formed in the submonolayer regime, e.g., before a complete layer is formed. For example, sputter deposition of Al, Cu, and Cr (Refs. 11 and 12) on amorphous SiO<sub>2</sub> and TiO<sub>2</sub> as well as plasma-enhanced chemical vapor deposition (PECVD) of hydrogenated amorphous Si on SiO<sub>2</sub> (Refs. 13 and 14) can lead to nonwetting 3D island growth. Therefore, understanding the scaling behavior of the island density and size distribution in the case of 3D island growth is of interest.

We note that in the case of 3D island growth a distinction should be made between the coverage  $\theta$  corresponding to the substrate area fraction covered by islands and the dose  $\phi$  corresponding to the number of particles per unit area [or equivalent monolayers (ML)] deposited. In particular, since the onset of island coalescence is related to the coverage  $\theta$  we expect that the scaling of the peak island density is equivalent to that of the island density at fixed coverage. Based on this assumption, standard nucleation theory<sup>2,3</sup> pre-

dicts that for 3D island growth, the effective value of the exponent describing the flux dependence of the peak island density is given by  $\chi'_i = \frac{i}{i+2.5}$  rather than  $\chi_i = \frac{i}{i+2}$  as for 2D islands. This relation has been used to analyze the dependence of the peak 3D island density on temperature and flux in a number of experimental papers.<sup>15,16</sup> However, while there have been many studies of 2D island growth, there have been few theoretical<sup>17</sup> studies of the scaling behavior of the island density and ISD for 3D islands.

Here we present the results of simulations of a simple model of 3D irreversible island growth, carried out in order to better understand the relevant scaling behavior in this case. We have also compared our results for the scaled island-size distribution with those obtained for 2D islands. In addition to our simulations, we also present a general theoretical relation (valid for any critical island size) connecting the exponent  $\chi_i$  corresponding to the flux dependence of the island density at fixed dose  $\phi$  and the exponent  $\chi'_i$  corresponding to the flux dependence of the peak island density. For comparison with our simulation results we also present self-consistent rate-equation (RE) results for the island and monomer densities as a function of coverage. Since our simulations are motivated in part by recent experiments on amorphous-Si grown via PECVD for which it was found that there is a large wetting angle,<sup>13,18</sup> here we assume that the 3D islands are hemispherical rather than faceted. In addition, since strain due to island-substrate lattice mismatch is unlikely to play a role in the growth of a-Si islands, the effects of strain are not included in our model.

In qualitative agreement with the standard RE prediction, we find that (in contrast to the case of 2D islands) for 3D islands the island density does not saturate with increasing coverage in the precoalescence regime. Accordingly, the effective value of  $\chi'_i$  is indeed somewhat smaller than the value ( $\chi_1=1/3$ ) for 2D irreversible island growth. However, due to the fact that the average capture number for 3D islands increases with coverage, some deviations are also observed. For example, the effective values of the exponents  $y_1$  and  $y'_1$  describing the dependence of the island density on dose  $\phi$  and coverage  $\theta$  in the precoalescence regime are significantly smaller than the standard RE prediction. As a result, the value of  $\chi'_1$  obtained in our simulations ( $\chi'_1 \approx 0.30$ ) is somewhat larger than the standard RE theory prediction ( $\chi'_1 = 2/7 \approx 0.286$ ). We also find good agreement between the results of a self-consistent RE calculation and our simulation results for the island and monomer densities as a function of coverage/dose and  $D/F$ . However, despite these differences we find very little difference between the scaled ISD for 3D islands and that for 2D islands.

In addition to these results, we also discuss the dependence of the exponent  $\chi'_i$  on the critical island size  $i$ . However, since  $\chi'_i$  depends only weakly on  $y'_i$ , this only leads to small deviations from the standard RE predictions for  $\chi'_i$ . Finally, we discuss the suitability of measuring the exponents  $y_i$  (or  $y'_i$ ) rather than  $\chi'_i$  in order to estimate the critical island size.

This paper is organized as follows. In Sec. II, we first describe our model while in Sec. III, we describe the self-consistent rate-equation approach. In Sec. IV we first use a scaling approach to derive general expressions connecting

the exponent  $\chi_i$  corresponding to the scaling of the island density at fixed dose  $\phi$  and the exponent  $\chi'_i$  corresponding to the scaling of the island density at fixed coverage. We then compare our simulation results with the predictions of this scaling approach, as well as with our self-consistent RE results. A comparison between the scaled ISD for 2D and 3D islands is also presented. Finally, in Sec. V we summarize our results.

## II. MODEL

Since our simulations are motivated, in part, by recent experiments on amorphous Si grown via PECVD for which it was found that there is a large wetting angle<sup>13,18</sup> here we assume for simplicity that the 3D islands are hemispherical while a substrate consisting of a square lattice of deposition sites with lattice constant  $a$  is also assumed for simplicity. Accordingly, each island of size  $s$  is represented by a hemisphere with volume  $v_s = 2\pi r_s^3/3$  and radius  $r_s = r_1 s^{1/3}$ , where  $r_1 = a/2$ . While such an assumption is not entirely realistic for small islands, we do not expect that inclusion of a more realistic size dependence for small islands will affect the results presented here since the asymptotic scaling behavior is determined by the large islands.

In order to take deposition into account, in our model atoms are randomly deposited onto the substrate with rate  $F$  per unit time per lattice site while monomers are assumed to hop in each of the four nearest-neighbor directions with hopping rate  $D_h = D/4$ , where  $D$  is the total hopping rate. Since we are assuming irreversible growth, when two monomers are nearest neighbors they are assumed to form a stable dimer while any monomers which overlap with an island either via direct impingement or via diffusion are assumed to aggregate irreversibly to the island. In particular, we assume that when two monomers become nearest neighbors they form a hemisphere with radius  $r_2$  whose center is located at the center of mass of the two monomers. Similarly, if a monomer overlaps with an island, then the monomer is “absorbed” and the radius of the island is increased accordingly. Although the focus here is on the precoalescence regime, we also assume that if two islands overlap then a third island is formed by the “union” of the two initial islands. In this case, the radii of the islands are also adjusted to ensure mass conservation.

For comparison, we have also carried out similar simulations for the case of 2D circular islands. In this case, everything is the same as for the 3D case except that the island area and radius are given by the expressions  $a_s = \pi r_s^2$  and radius  $r_s = r_1 s^{1/2}$  with  $r_1 = a/2$  as before. In order to avoid finite-size effects, in our kinetic Monte Carlo (KMC) simulations we have used a large system size of  $1024 \times 1024$  lattice sites while averages over 100 runs were taken to obtain good statistics. In order to determine the asymptotic dependence of the island density on coverage and  $D/F$  our simulations were carried out using values of  $D/F$  ranging from  $10^9 - 10^{11}$  up to a maximum coverage of 0.2 ML.

## III. SELF-CONSISTENT RATE-EQUATION APPROACH

For comparison with our simulations we have also carried out self-consistent RE calculations following the method

originally developed by Bales and Chrzan.<sup>19</sup> We note that while this method<sup>19–21</sup> does not give accurate results for the island-size distribution, it is expected to give accurate results for the average island and monomer densities  $N(\theta)$  and  $N_1(\theta)$ . In particular, in the case of 3D islands our rate equations may be written in the following form:

$$\frac{dN_1}{d\phi} = 1 - 2R\sigma_1 N_1^2 - RN_1 \sum_{s=2}^{\infty} \sigma_s N_s - \kappa_1 N_1 - \sum_{s=1}^{\infty} \kappa_s N_s \quad (3)$$

$$\frac{dN_s}{d\phi} = RN_1(\sigma_{s-1} N_{s-1} - \sigma_s N_s) - \kappa_{s-1} N_{s-1} - \kappa_s N_s \quad (s \geq 2), \quad (4)$$

where  $\phi$  is the deposited dose in ML,  $R=D/F$  is the ratio of the monomer diffusion rate  $D$  to the (per site) deposition rate  $F$ , the terms with  $\kappa_s$  correspond to direct impingement of atoms deposited on top of islands, and the capture numbers  $\sigma_s$  ( $\sigma_1$ ) correspond to the average capture rate of diffusing monomers by islands of size  $s$  (monomers).

In order to numerically integrate the REs above we need to know the size dependence and dose dependence of the relevant capture numbers  $\sigma_s(\phi)$ . In order to do so we consider a quasistatic diffusion equation for the monomer density  $n_1(r, \tilde{\phi})$  surrounding an island of size  $s$  of the form

$$\nabla^2 n_1(r, \tilde{\phi}) - \xi^{-2}(n_1 - N_1) = 0, \quad (5)$$

where  $N_1$  is the average monomer density and  $\xi$  is the average capture length. Assuming circular symmetry and solving for  $n_1(r)$ , using the boundary conditions  $n_1(\infty) = N_1$  and  $n_1(\tilde{r}_s) = 0$  (where  $\tilde{r}_s = r_s + r_1$  is the effective monomer capture radius of an island of size  $s$ ) the following expression for the capture number can be obtained:<sup>19</sup>

$$\sigma_s = 2\pi \frac{\tilde{r}_s K_1(\tilde{r}_s/\xi)}{\xi K_0(\tilde{r}_s/\xi)}, \quad (6)$$

where the  $K_j$  are modified Bessel functions of order  $j$ . Similarly, the monomer capture radius  $\tilde{r}_s$  can be used to calculate the direct impingement term, e.g.,  $\kappa_s = \pi \tilde{r}_s^2$ . We note that in our self-consistent RE calculations inclusion of the monomer capture radius  $r_1$  in the definition of  $\tilde{r}_s$  turns out to be crucial to obtain good quantitative agreement with our simulations.

For consistency with the REs [Eqs. (3) and (4)] we require

$$\xi^{-2} = 2\sigma_1 N_1 + \sum_{s=2}^{\infty} \sigma_s N_s. \quad (7)$$

Thus, for a given dose  $\phi$  and island-size distribution  $N_s(\phi)$ , the capture-length  $\xi$  may be determined self-consistently starting with an initial guess for  $\xi$  in Eq. (6) and then substituting into Eq. (7) and repeating until the process converges.

#### IV. RESULTS

##### A. Scaling approach to 3D island growth

Before presenting our simulation results, we first consider the standard RE approach for the flux dependence and dose

dependence of the island density for a given critical island-size  $i$ . In particular, assuming size- and coverage-independent capture numbers  $\sigma$  one may write the following truncated rate equations for the densities  $N(N_1)$  of stable islands (monomers):

$$\frac{dN}{d\phi} = \sigma RN_1 N_i, \quad (8)$$

$$\frac{dN_1}{d\phi} = 1 - 2\sigma RN_1^2 - 2\kappa_1 N_1 - \sum_{s \geq 2} \kappa_s N_s - \left( \sigma RN_1 - \frac{\delta_s}{F} \right) \sum_{s=2}^i N_s - \sigma RN_1 N, \quad (9)$$

where  $N = \sum_{s \geq i+1} N_s$  and  $\delta_s$  corresponds to the monomer detachment rate for an island of size  $s$ . In the limit of large  $D/F$  and beyond the nucleation regime the first and last terms in Eq. (9) dominate and  $dN_1/d\phi \approx 0$  which implies

$$N_1 \sim (RN)^{-1}. \quad (10)$$

Assuming the Walton relation<sup>1</sup>  $N_i \sim N_1^i e^{E_b/k_B T}$  (where  $E_b$  is the binding energy of the critical nucleus), and substituting Eq. (10) into Eq. (8) and solving for  $N$  we obtain

$$N \sim R^{-i/(i+2)} \phi^{1/(i+2)} e^{E_b/(i+2)k_B T}, \quad (11)$$

which implies that  $N \sim F^{\chi_i} \phi^{y_i}$ , where

$$\chi_i = i/(i+2), \quad y_i = 1/(i+2). \quad (12)$$

We note that this expression for  $\chi_i$  has been verified in many simulations of 2D submonolayer island growth.<sup>8,9,22,23,25</sup> However, the result for  $y_i$  has only been found to be valid for point islands.<sup>22,23</sup> In contrast—due to the fact that the average capture number and impingement terms increase with increasing coverage—for 2D islands the island density saturates with increasing coverage and one has  $y_i = 0$ .

We now consider the standard RE prediction for the exponents  $y'_i$  and  $\chi'_i$  describing the coverage dependence and flux dependence (at constant coverage), respectively, of the island density for 3D islands. In particular, one may write

$$\theta \sim NS^{2/3} \sim N(\phi/N)^{2/3} \sim N^{1/3} \phi^{2/3}, \quad (13)$$

where  $S = \phi/N$  is the average island size. Substituting into Eq. (11) we obtain

$$N \sim F^{2\chi_i/(y_i+2)} \theta^{3y_i/(y_i+2)} \sim F^{\chi'_i} \theta^{y'_i}, \quad (14)$$

which implies that

$$\chi'_i = 2\chi_i/(y_i+2), \quad y'_i = 3y_i/(y_i+2). \quad (15)$$

Substituting the expressions for  $\chi_i$  and  $y_i$  in Eq. (12) this result leads to the standard RE prediction for the flux dependence of the peak island density for 3D islands,<sup>24</sup>

$$\chi'_i = \frac{i}{i+2.5} \quad (16)$$

as well as the result,

TABLE I. Standard RE predictions for exponents as function of critical island size.

$i$	$\gamma_i$	$y_i$	$y'_i$	$\chi_i$	$\chi'_i$
1	0.778	0.333	0.429	0.333	0.286
2	0.750	0.250	0.333	0.500	0.444
3	0.733	0.200	0.273	0.600	0.545
4	0.722	0.167	0.231	0.667	0.615
5	0.714	0.143	0.200	0.714	0.667
6	0.708	0.125	0.176	0.750	0.706
7	0.704	0.111	0.158	0.778	0.737
8	0.700	0.100	0.143	0.800	0.762

$$y'_i = \frac{3}{5 + 2i}. \tag{17}$$

Substituting Eq. (11) into Eq. (13) and inverting to obtain  $\theta(\phi)$  we also obtain the following expression for the coverage  $\theta$  as a function of dose  $\phi$  in the case of 3D islands:

$$\theta \sim R^{-\chi_i/3} \phi^{\gamma_i}, \tag{18}$$

where  $\gamma_i = (y_i + 2)/3$ . We note that in the case of irreversible growth, Eq. (14) implies  $\theta \sim \phi^{7/9} \approx \phi^{0.778}$ . Table I shows a summary of the exponents  $\gamma_i, y_i, y'_i, \chi_i$  and  $\chi'_i$  as a function of critical island size  $i$  for  $i = 1 - 8$ . As can be seen, except for the exponent  $\gamma_i$  all of the other exponents depend sensitively on the critical island size.

**B. Simulation results**

We first consider the dependence of the island and monomer densities on dose  $\phi$  for the case of irreversible growth of 3D (hemispherical) islands. As can be seen in Fig. 1(a), in contrast to the case of 2D islands [see Fig. 3(b)] for which the island density saturates at doses less than 1 ML, for 3D islands the saturation dose is much higher than 1 ML since the effective coverage is reduced. Also shown in Fig. 1(a) are our self-consistent RE results (solid curve). As can be seen, there is very good agreement with our simulation results. However, a power-law fit to the dependence of the island density on dose in the pre-coalescence regime [see Fig. 1(b)] gives an effective value ( $y_1 \approx 0.24$ ) which is significantly lower than the standard RE prediction given by Eq. (12) ( $y_1 = 1/3$ ). In contrast, fits for the island density at constant dose as a function of  $D/F$  (not shown) give a value  $\chi_1 \approx 0.32$  in good agreement with the standard prediction of  $1/3$ .

We now consider the dependence of the island density on coverage. As can be seen in Fig. 2(a), the island density (solid curves) saturates at a coverage slightly above 0.1 ML. As indicated by the continued increase in the total density of nucleated islands (dashed curve) this saturation is due to coalescence. In addition, fits to the coverage dependence in the pre-coalescence regime [see Fig. 2(b)] give a value of  $y'_1$  ( $y'_1 \approx 0.32$ ) which is significantly lower than the standard RE prediction ( $y'_1 = 3/7 \approx 0.43$ ) although in good agreement with the value obtained using Eq. (15) if we assume the measured

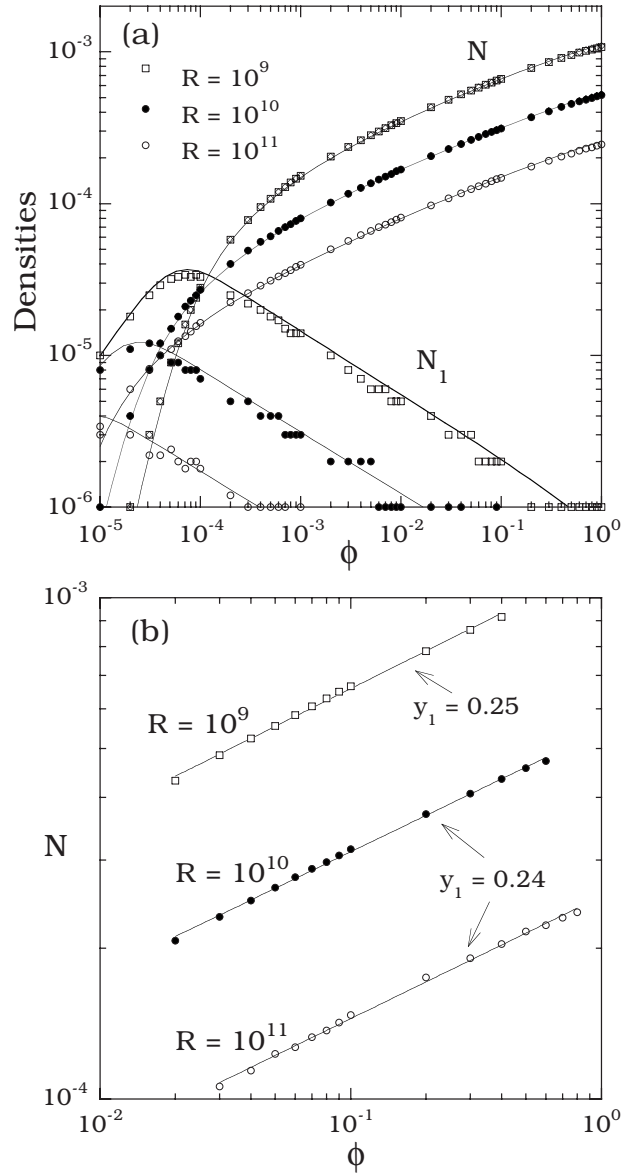


FIG. 1. (a) Island density  $N$  and monomer density  $N_1$  as a function of dose  $\phi$  obtained from KMC simulations (symbols) and self-consistent RE calculations (solid curves) for  $D/F = 10^9 - 10^{11}$ . (b) Island density as a function of dose showing power-law behavior beyond the nucleation regime.

value of  $y_1$  ( $y_1 \approx 0.24$ ) rather than the predicted value ( $y_1 = 1/3$ ). Also shown in Fig. 2(a) (inset) is a plot of the island density at fixed coverage ( $\theta = 0.07$ ) in the pre-coalescence regime as a function of  $D/F$ . As can be seen the effective value of the island-density scaling exponent obtained in our simulations ( $\chi'_1 \approx 0.30$ ) is slightly higher than the standard RE prediction ( $\chi'_1 = 2/7 \approx 0.286$ ) but still somewhat lower than the value ( $1/3$ ) expected for 2D islands.

In order to further understand the difference between the coverage dependence and dose dependence of the island density for 3D islands, in Fig. 3(a) we show the dependence of the coverage  $\theta$  on dose  $\phi$  obtained in our simulations. As can be seen, the dependence of coverage on dose exhibits power-law behavior, e.g.,  $\theta \sim \phi^\gamma$  over the entire range of dose, with an exponent  $\gamma_1 \approx 0.76$  which is somewhat smaller than the

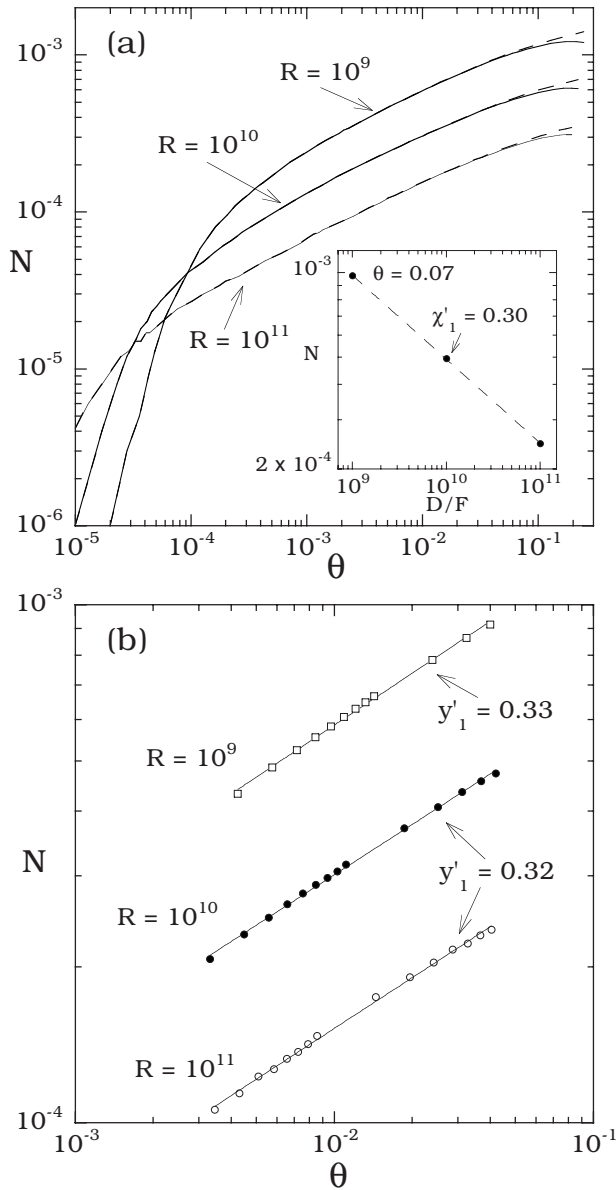


FIG. 2. (a) Island density  $N$  and monomer density  $N_1$  as a function of coverage  $\theta$  obtained from KMC simulations (solid curves) for  $D/F=10^9-10^{11}$ . Dashed line corresponds to density of nucleated islands (see text). Inset shows  $D/F$  dependence of island density at fixed coverage. (b) Island density as a function of coverage showing power-law behavior beyond the nucleation regime.

standard RE prediction  $\gamma_1=7/9 \approx 0.78$  but in good agreement with the expression  $\gamma_1=(y_1+2)/3$  given in Eq. (14) if we assume  $y_1=0.24$ . For comparison, simulation results for the island density as a function of coverage for 2D circular islands are shown in Fig. 3(b) up to a coverage  $\theta=0.5$  ML. As can be seen, the saturation coverage is close to that for 3D islands. In addition, we again find excellent agreement in the pre-coalescence regime ( $\theta < 0.1$  ML) between our self-consistent RE results (curved lines) and simulation results.

Finally, we compare the submonolayer morphology and scaled island-size distribution for 2D and 3D islands. Figure 4 shows typical pictures for [(a)–(c)] 3D and [(d)–(f)] 2D islands at  $\theta=0.07$  ML and  $D/F=10^9-10^{11}$ . As expected,

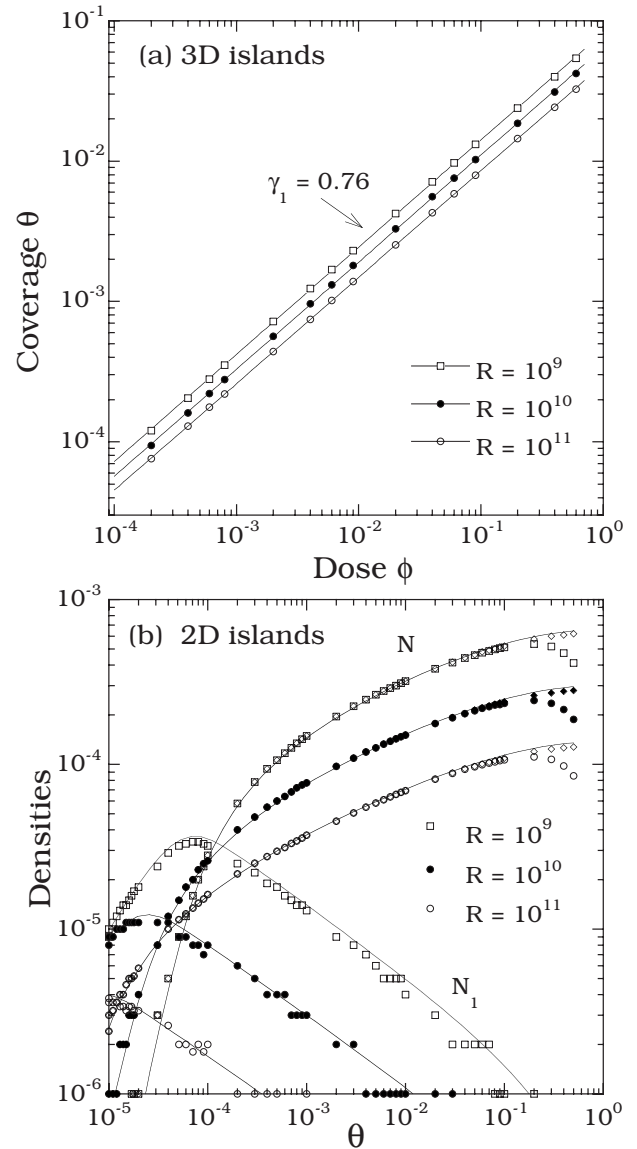


FIG. 3. (a) Log-log plot of coverage  $\theta$  as a function of dose  $\phi$  for 3D islands for  $D/F=10^9-10^{11}$  (b) Island density  $N$  and monomer density  $N_1$  for 2D islands as a function of coverage  $\theta$  for  $D/F=10^9-10^{11}$ . Symbols correspond to KMC results while solid curves correspond to results of self-consistent RE calculations. Small diamonds correspond to density of nucleated islands (ignoring coalescence) while larger symbols correspond to total island density.

with increasing  $D/F$  the island density decreases while the average island size increases. However, due to the fact that the capture number for 2D islands is larger than that for 3D islands, the island density is much lower for 2D islands than for 3D islands.

Figure 5 shows the corresponding results for the scaled ISD for 2D and 3D islands. As can be seen, there is very good scaling behavior as a function of  $D/F$  while there is very little difference between the scaled ISD for 2D and 3D islands. We also note that the scaled ISD obtained in our simulations in the pre-coalescence regime ( $\theta=0.07$  ML) is very similar to that obtained in previous simulations of the irreversible growth of compact (square) 2D islands.<sup>25</sup> In par-

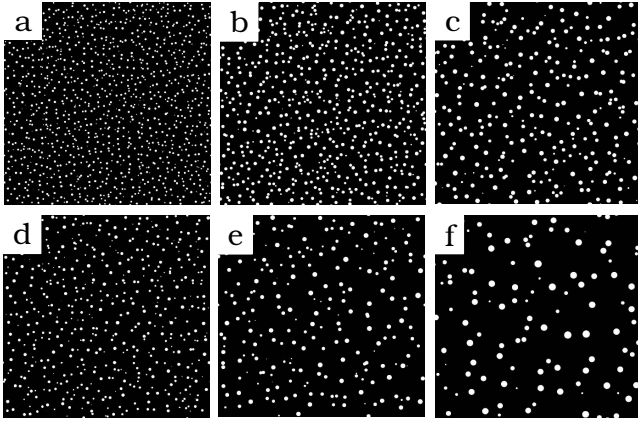


FIG. 4. Comparison of morphology at coverage  $\theta=0.07$  for [(a)–(c)] 3D islands and [(d)–(f)] 2D islands. System-size  $L=1024$  while from left to right,  $D/F=10^9$ ,  $10^{10}$ , and  $10^{11}$ .

ticular, in the pre-coalescence regime the peak of the ISD is slightly shifted to the right from  $s/S=1$  while the value of  $f(0)$  [ $f(0)\approx 0.4$ ] is somewhat larger than the standard point-island prediction [ $f(0)\approx 1/3$ ]. In contrast, if we consider the scaled ISD at fixed dose (not shown) and increasing values of  $D/F$ , poor scaling behavior is found since the coverage decreases with increasing  $D/F$ .

## V. DISCUSSION

In order to understand the scaling behavior of the island density and island-size distribution in irreversible 3D island growth, we have carried out kinetic Monte Carlo simulations of a simplified model. For comparison we have also derived general expressions based on a mean-field RE analysis, for the exponents  $y_i$  describing the dose dependence,  $y'_i$  describing the coverage dependence, and  $\chi'_i$  describing the  $D/F$

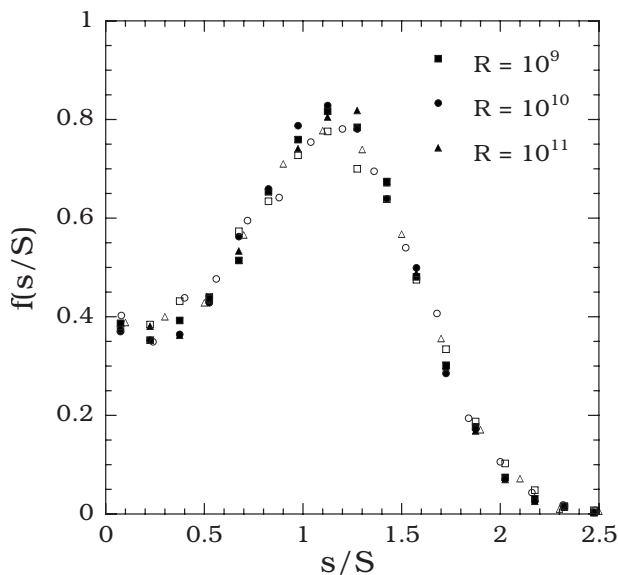


FIG. 5. Comparison of scaled ISD for 3D islands (filled symbols) and 2D islands (open symbols) at  $\theta=0.07$  ML for  $D/F=10^9-10^{11}$ .

dependence (at fixed coverage) of the island density as a function of critical island size  $i$ . We note that, since the onset of coalescence is determined by the coverage, the exponent  $\chi'_i$  also describes the dependence of the peak island density on  $D/F$ . A general expression for the exponent  $\gamma_i$  describing the dependence of coverage on dose has also been derived.

In contrast to the standard RE predictions ( $y_1=1/3$ ,  $y'_1=3/7\approx 0.43$ ) for 3D irreversible growth,<sup>2</sup> we find significantly lower values ( $y_1\approx 0.24$ ,  $y'_1\approx 0.32$ ) for the effective exponents describing the dose dependence and coverage dependence of the island density for 3D islands. This may be explained by the fact that, in contrast to the standard RE assumption of size-independent capture numbers, for 3D islands the island radius increases with the number of atoms in an island. Accordingly, the average capture number also increases with coverage, thus leading to a decrease in the rate of nucleation as well as the effective exponents  $y_1$  and  $y'_1$  describing the increase in the island density in the pre-coalescence regime. We note that a similar effect occurs in 2D island growth.<sup>8,23</sup> However, in this case the strong increase in the average capture number with island size leads to saturation of the island density. As a result, the coverage dependence of the island density for 3D islands is intermediate between that for 2D islands (for which  $y_1=0$ ) and the standard RE prediction based on the assumption of size-independent capture numbers. This behavior should be contrasted with that obtained for point islands (for which the ratio  $\bar{r}/l$  of the average island radius  $\bar{r}$  to the average island distance  $l$  is small and approaches 0 with increasing  $D/F$ ) for which the value of  $y_1$  obtained in simulations<sup>25</sup> ( $y_1\approx 0.33$ ) is in good agreement with the standard RE prediction.

Our results also indicate that the value of  $\chi'_1$  ( $\chi'_1\approx 0.30$ ) for 3D islands lies in between the value for 2D islands ( $\chi_1=\chi'_1=1/3$ ) and the standard RE prediction ( $\chi'_1=1/3.5\approx 0.29$ ). This value of  $\chi'_1$  is also consistent with Eq. (15) and the value of  $y_1$  obtained in our simulations. However, since the exponent  $\gamma_1$  depends only weakly on  $y_1$  [e.g.,  $\gamma_1=(y_1+2)/3$ ], and  $y_1$  is significantly less than 1, the resulting “correction” to  $y_1$  leads to only a very small change in the exponent  $\gamma_1$  (e.g.,  $\gamma_1\approx 0.76$  rather than the expected value  $\gamma_1=7/9\approx 0.78$ ).

For comparison, we have also carried out self-consistent RE calculations and good agreement was found between our RE results for the island and monomer densities and our KMC results. It is worth noting that, in contrast to previous work<sup>19,25</sup> on square and fractal islands in which an adjustable factor which scales the overall island radius was needed to take into account geometrical effects, in this case good agreement was obtained without any adjustable parameters. This is most likely due to the fact that the circular island geometry assumed in our simulations is consistent with that assumed in the self-consistent RE approach.

We have also presented a comparison of results for the island density and scaled ISD for 2D and 3D irreversible island growth. Since the average capture number is smaller for 3D islands, the island density is significantly larger (for the same value of  $D/F$ ) than for 2D islands. However, somewhat surprisingly, we find that there is very little difference between the scaled ISD for 3D islands and that for 2D islands. This indicates that, as previously found in simulations

of 2D submonolayer island growth,<sup>9</sup> the scaled ISD is primarily determined by the critical island size rather than the island morphology. We note that this result is also consistent with a previous analysis<sup>26</sup> of experimental results for InGaAs/GaAs growth,<sup>27</sup> which indicates a small critical island size for the formation of 2D platelets.

While our simulation results clearly indicate that for typical values of  $D/F$  the scaling behavior deviates from the standard RE predictions, it is also of interest to consider the asymptotic limit of infinite  $D/F$ . In this connection, we note that for point islands (for which the ratio  $\bar{r}/l$  of the average island radius  $\bar{r}$  to the average island distance  $l$  is small) the value of  $y_1$  obtained in simulations<sup>25</sup> ( $y_1 \approx 0.33$ ) is in good agreement with the standard RE prediction. We therefore expect that if  $\bar{r}/l$  goes to zero in the limit of large  $D/F$ , then the asymptotic scaling behavior will be the same as for point islands. However, in general one may write  $\bar{r} \sim (\theta/N)^{1/2}$  (where  $\theta/N$  is the average area per island) and  $l \sim N^{-1/2}$  which implies  $\bar{r}/l \sim \theta^{1/2}$ . This implies that in the asymptotic limit of large  $D/F$ , the ratio  $\bar{r}/l$  remains independent of  $D/F$  and only depends on the coverage. As a result, we expect that the deviations from standard RE theory found in our simulations for  $D/F=10^9-10^{12}$  will also occur for higher values of  $D/F$ . This is consistent with our observation that with increasing  $D/F$  the exponents  $y_1$  and  $y_1'$  do not approach the standard RE values.

Finally, we consider the general problem of experimentally determining the critical island size in 3D island growth. As already noted, except for the exponent  $\gamma_i$  describing the

dependence of the coverage on dose (or time) all of the other exponents depend sensitively on the critical island size. In addition, since the exponent  $\chi_i'$  depends only weakly on the dynamic exponent  $y_i$  [see Eq. (15)] deviations from the standard RE theory for 3D islands are likely to be relatively small compared to the dependence on  $i$  (see Table I). This is consistent with the fact that our measured value of  $\chi_1'$  (0.30) is close to the standard RE prediction  $\chi_1' \approx 0.286$ . As a result, a direct determination of  $\chi_i'$ , by measuring the peak island density as a function of deposition flux, is still the most accurate method to determine the critical island size. However, such a measurement requires carrying out several growth experiments with different fluxes and in some cases it may be difficult to control the deposition flux. In this case, our results indicate (see Table I) that in contrast to the case of 2D islands (for which  $y_i=0$ ) for 3D islands an upper bound to the critical island size may be determined from a single experiment by measuring the exponent  $y_i$  describing the time dependence of the island density.

## ACKNOWLEDGMENTS

This work was supported in part by the Ohio Department of Development through the Wright Center for Photovoltaics Innovation and Commercialization (PVIC) at the University of Toledo. J.G.A. would also like to acknowledge support from NSF under Grant No. DMR-0907399. We would also like to acknowledge grants of computer time from the Ohio Supercomputer Center (Grant No. PJS0245).

\*yevgen.kryukov@utoledo.edu

†jamar@physics.utoledo.edu

<sup>1</sup>D. Walton, *J. Chem. Phys.* **37**, 2182 (1962); D. Walton, T. N. Rhodin, and R. W. Rollins, *ibid.* **38**, 2698 (1963).

<sup>2</sup>J. A. Venables, *Philos. Mag.* **27**, 697 (1973).

<sup>3</sup>J. A. Venables, G. D. Spiller, and M. Hanbucken, *Rep. Prog. Phys.* **47**, 399 (1984).

<sup>4</sup>R. Kunkel, B. Poelsema, L. K. Verheij, and G. Comsa, *Phys. Rev. Lett.* **65**, 733 (1990).

<sup>5</sup>Z. Y. Zhang and M. G. Lagally, *Science* **276**, 377 (1997).

<sup>6</sup>For a review see, J. W. Evans, P. A. Thiel, and M. C. Bartelt, *Surf. Sci. Rep.* **61**, 1 (2006).

<sup>7</sup>J. W. Evans and M. C. Bartelt, *J. Vac. Sci. Technol. A* **12**, 1800 (1994).

<sup>8</sup>J. G. Amar, F. Family, and P. M. Lam, *Phys. Rev. B* **50**, 8781 (1994).

<sup>9</sup>J. G. Amar and F. Family, *Phys. Rev. Lett.* **74**, 2066 (1995).

<sup>10</sup>V. A. Shchukin and D. Bimberg, *Rev. Mod. Phys.* **71**, 1125 (1999).

<sup>11</sup>Ji-Yong Park, S.-J. Kahng, U. D. Ham, Y. Kuk, K. Miyake, K. Hata, and H. Shigekawa, *Phys. Rev. B* **60**, 16934 (1999).

<sup>12</sup>M. Hu, S. Noda, and H. Komiyamar, in *Nanostructured and Patterned Materials for Information Storage*, edited by Z. Z. Bandic, M. Rooks, R. Berger, and T. Ando, MRS Symposia Proceedings No. 961 (Materials Research Society, Pittsburgh, 2007), p. 0961-O05-05.

<sup>13</sup>H. Kanai, S. Sugihara, H. Yamaguchi, T. Uchimaru, N. Obata,

T. Kikuchi, F. Kimura, and M. Ichinokura, *J. Mater. Sci.* **42**, 9529 (2007).

<sup>14</sup>R. W. Collins, A. S. Ferlauto, G. M. Ferreira, Chi Chen, Joohyun Koh, R. J. Koval, Yeeheng Lee, J. M. Pearce, and C. R. Wronski, *Sol. Energy Mater. Sol. Cells* **78**, 143 (2003).

<sup>15</sup>J. S. Sullivan, H. Evans, D. E. Savage, M. R. Wilson, and M. G. Lagally, *J. Electron. Mater.* **28**, 426 (1999).

<sup>16</sup>T. Schlenker, H. W. Schock, and J. H. Werner, *J. Cryst. Growth* **259**, 47 (2003).

<sup>17</sup>J. Dalla Torre, G. H. Gilmer, and M. Djafari Rouhani, *Phys. Rev. B* **69**, 195414 (2004).

<sup>18</sup>Y. A. Kryukov, N. J. Podraza, R. W. Collins, and J. G. Amar, *Phys. Rev. B* **80**, 085403 (2009).

<sup>19</sup>G. S. Bales and D. C. Chrzan, *Phys. Rev. B* **50**, 6057 (1994).

<sup>20</sup>F. Shi, Y. Shim, and J. G. Amar, *Phys. Rev. B* **71**, 245411 (2005).

<sup>21</sup>F. Shi, Y. Shim, and J. G. Amar, *Phys. Rev. E* **74**, 021606 (2006).

<sup>22</sup>M. C. Bartelt and J. W. Evans, *Phys. Rev. B* **46**, 12675 (1992).

<sup>23</sup>C. Ratsch, A. Zangwill, P. Smilauer, and D. D. Vvedensky, *Phys. Rev. Lett.* **72**, 3194 (1994).

<sup>24</sup>J. A. Venables, *Surf. Sci.* **299-300**, 798 (1994).

<sup>25</sup>M. N. Popescu, J. G. Amar, and F. Family, *Phys. Rev. B* **64**, 205404 (2001).

<sup>26</sup>Y. Chen and J. Washburn, *Phys. Rev. Lett.* **77**, 4046 (1996).

<sup>27</sup>D. Leonard, K. Pond, and P. M. Petroff, *Phys. Rev. B* **50**, 11687 (1994).